Operation of Stand Alone PV Generating System for Supplying Unbalanced AC Loads

R. Noroozian*, M. Abedi*, G. B. Gharehpetian* and S. H. Hosseini**

Abstract: This paper describes a DC isolated network which is fed with Distributed Generation (DG) from photovoltaic (PV) renewable sources for supplying unbalanced AC loads. The battery energy storage bank has been connected to the DC network via DC/DC converter to control the voltage of the network and optimize the operation of the PV generation units. The PV arrays are connected to the DC network via its own DC/DC converter to ensure the required power flow. The unbalanced AC loads are connected to the DC network via its own DC/AC converter. This paper proposes a novel control strategy for storage converter which has a DC voltage droop regulator. Also a novel control system based on Park rotating frame has been proposed for DC/AC converters. In this paper, the proposed operation method is demonstrated by simulation of power transfer between PV arrays, unbalanced AC loads and battery unit. The simulation results based on PSCAD/EMTDC software show that DC isolated distribution system including PV generation systems can provide the high power quality to supplying unbalanced AC loads.

Keywords: Distributed Generation, Photovoltaic, Power Control, Power Quality, Stand Alone System, Strategy Control.

1 Introduction

Renewable energy resources are attractive options for supplying loads in places where a connection to the utility network is either impossible or unduly expensive [1]. However, small isolated PV generation units can feed local loads in many of the remote areas, and thus improve reliability of power with low capital investment [2]. In general, PV units are operated as a stand alone, a grid configuration or hybrid system. Stand alone (off-grid) PV units has been defined as the combination of PV arrays, battery bank and AC and DC loads. Power generated in the stand alone PV array can be supplied for corresponding load. As a result, isolated PV generation units have battery banks to compensate the difference between load power and generated power. However, daytime operating mode, when the PV power is larger than the load demand, the power is supplied to the loads and would charge the battery bank. Nighttime operating mode, the PV power is absent and the battery bank supplies the loads. Additionally, if the generated power is greater than the load demand while the battery bank is fully charged the excessive power has been existed. To overcome this problem, the share of power between the battery bank and several PV generation units grid configuration is studied [3]. In this paper, the modeling of stand alone PV generating system has been presented. The aim of this paper is supplying the unbalanced AC load in DC isolated network by a DC/AC load converter. The load converter should deliver constant balanced AC voltage magnitude and frequency. However, a novel proposed control system based on Park rotating frame has been proposed for load converters. In $d-q-0$ rotating frame, the load current and voltage components in the $d-q$ channels are given rise to 2ω current ripples. The zero component appears as a disturbance at ω [4-6]. These three sequences are regulated independently by the Proportional Integral (PI) controllers. Integration of PV generation units in DC isolated distribution systems provides high power quality for unbalanced AC loads. The results of the digital simulation show that the concept of the proposed system to share the power between battery bank and several PV arrays is established. One of the most important characteristics of this system is transferring the excess power by sharing the battery during different operating conditions. The rest of this paper is arranged as follows. Section 2 briefly describes the DC isolated distribution system study configuration. The power management strategies for the proposed system are discussed in Section 3.
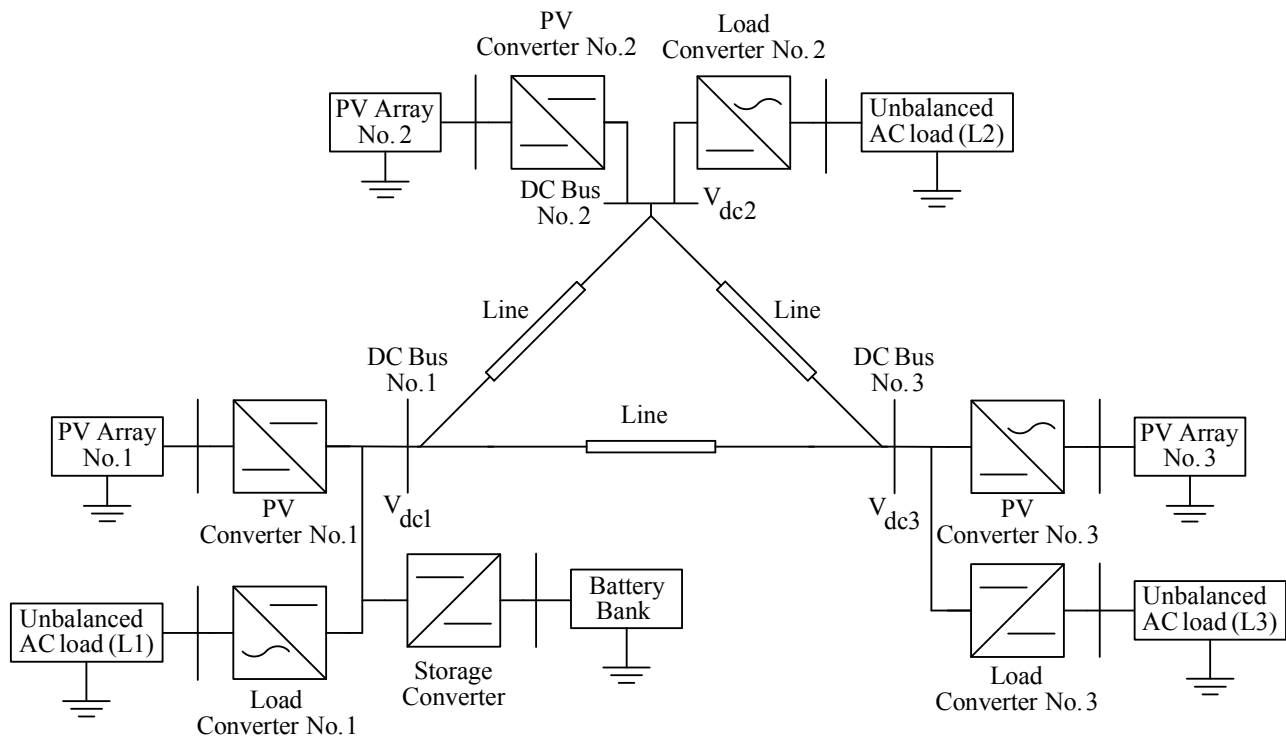
Fig. 1 The investigated DC isolated distribution system configuration.

Section 4 describes the control strategies of power electronic converters based on large-signal modeling. Simulation results of the proposed system are shown in Section 5.

2   DC Isolated Distribution System Configuration

Figure 1 shows the block diagram of a loop network configuration for DC isolated distribution system including PV arrays, unbalanced AC loads and one battery bank. This could be the model for a small off-grid distribution system. The proposed system should be able to transmit the power of PV arrays to the energy storage and load demand. Each DC bus is composed of photovoltaic array, DC/DC converter, unbalanced AC load and DC/AC converter. Distance among each PV arrays is 300 m, and each load consumes electrical energy from photovoltaic renewable sources that match the size of its own average consumption. It is assumed that the each PV array has the similar characteristics and location. A battery bank is connected the DC bus No. 1 via DC/DC converter, is called storage converter. The battery bank may be sized to cover the load connected to the DC network for different operating conditions. In Fig. 1, Each PV array has been connected in parallel by unbalanced AC load. Also each PV generation unit is connected to the DC network via the DC/DC converter, This DC/DC converter are called PV converter. Each unbalanced AC load is connected to the DC network via DC/AC converter. This DC/AC converter is called load converter. Power balancing in DC network could be achieved by bidirectional storage converter equipped with DC voltage regulator, which adjusts the DC

voltage at acceptable limit. In the sample system, using of suitable control strategy, it would be possible to share the load between the various PV arrays and the storage system. The proposed system is reliable, because the stored energy has two possibilities to flow from the battery bank to the loads.

3   Power Management of the Proposed System

Operation of the proposed system has been divided into three modes: daytime mode, nighttime mode, and daytime excess power transfer. The modes are shown in Fig. 2.

• Daytime mode: When the PV power is larger than the load demand throughout the system, the power is supplied to the loads and charged to the battery bank as shown in Fig. 2(a).

• Nighttime mode: The PV power is absent and only the battery bank supplies the loads as shown in Fig. 2(b).

• Daytime excess power transfer mode: When the output power in PV arrays No. 2 and No. 3 is lower than the load demand, and the power generated in PV array No. 1 is greater than the load demand, the shortage of power in PV arrays No. 2 and No. 3 is compensated by the excess power of PV array No. 1 without discharging the battery bank as shown in Fig. 2(c). Any excess power throughout the proposed system will be charged to the battery bank. If the available power is still insufficient to supply the load, the battery bank must be discharged to accommodate the load as shown in Fig. 2(d).

Power management strategy related to storage converter should provide the reference active power signals for the power regulation. The reference active power signal of the storage converter is determined by the DC voltage droop regulator system, which will be discussed in the next section. The reference active power of a PV unit is specified by its power management system which should consider various technical and economical constraints. The dynamic model for the DC side of the sample system is shown in Fig. 3. The storage converter can be modeled by current source controlled by DC bus voltage, while the PV converters are operating in the current control mode. The control philosophy for storage converter is based on feedback from the DC bus voltage, V_{dc1} and the reference value for the DC bus voltage. If the DC bus voltage is low, thus the power should be injected to the DC network by PV arrays, from the storage system. If the DC bus voltage is high, therefore the surplus power in DC network must be recharged the battery storage system. In Fig 3, we have:

$$I_b(s) = \frac{V_{dc,refb}(s) - \frac{\omega}{s + \omega} V_{dc1}(s)}{R_b} \tag{1}$$

$$I_b(s) + I_{PV1}(s) - I_{L1}(s) = C_1 s V_{dc1}(s) + \frac{V_{dc1}(s) - V_{dc2}(s)}{R + Ls} + \frac{V_{dc1}(s) - V_{dc3}(s)}{R + Ls} \tag{2}$$

$$I_{PV2}(s) - I_{L2}(s) = C_2 s V_{dc2}(s) + \frac{V_{dc2}(s) - V_{dc1}(s)}{R + Ls} + \frac{V_{dc2}(s) - V_{dc3}(s)}{R + Ls} \tag{3}$$

$$I_{PV3}(s) - I_{L3}(s) = C_3 s V_{dc3}(s) + \frac{V_{dc3}(s) - V_{dc1}(s)}{R + Ls} + \frac{V_{dc3}(s) - V_{dc2}(s)}{R + Ls} \tag{4}$$

where I_b, $V_{dc,refb}$ and R_b are the output current, DC voltage reference and equivalent resistance of storage converter, respectively. The measured DC bus voltage is low-pass filtered to attenuate voltage ripple and to enhance controller pole placement. ω_{lp} is the break-over frequency of the low pass filter (LPF). I_{PV1}, I_{PV2} and I_{PV3} are the output current of PV converters No. 1, No. 2 and No. 3, respectively. I_{L1}, I_{L2} and I_{L3} are the output current of the load converters No. 1, No. 2 and No. 3, respectively. V_{dc1}, V_{dc2} and V_{dc3} are the voltage of DC bus No. 1, No. 2 and No. 3 respectively. C_1, C_2 and C_3 are the equivalent capacitance of all converters connected in parallel of the DC bus No. 1, No. 2 and No. 3, respectively. R and L are resistance and inductance for each cable connected among DC bus No. 1, No. 2 and No. 3. The distance between each PV array is equal.

(a)

(b)

(c)
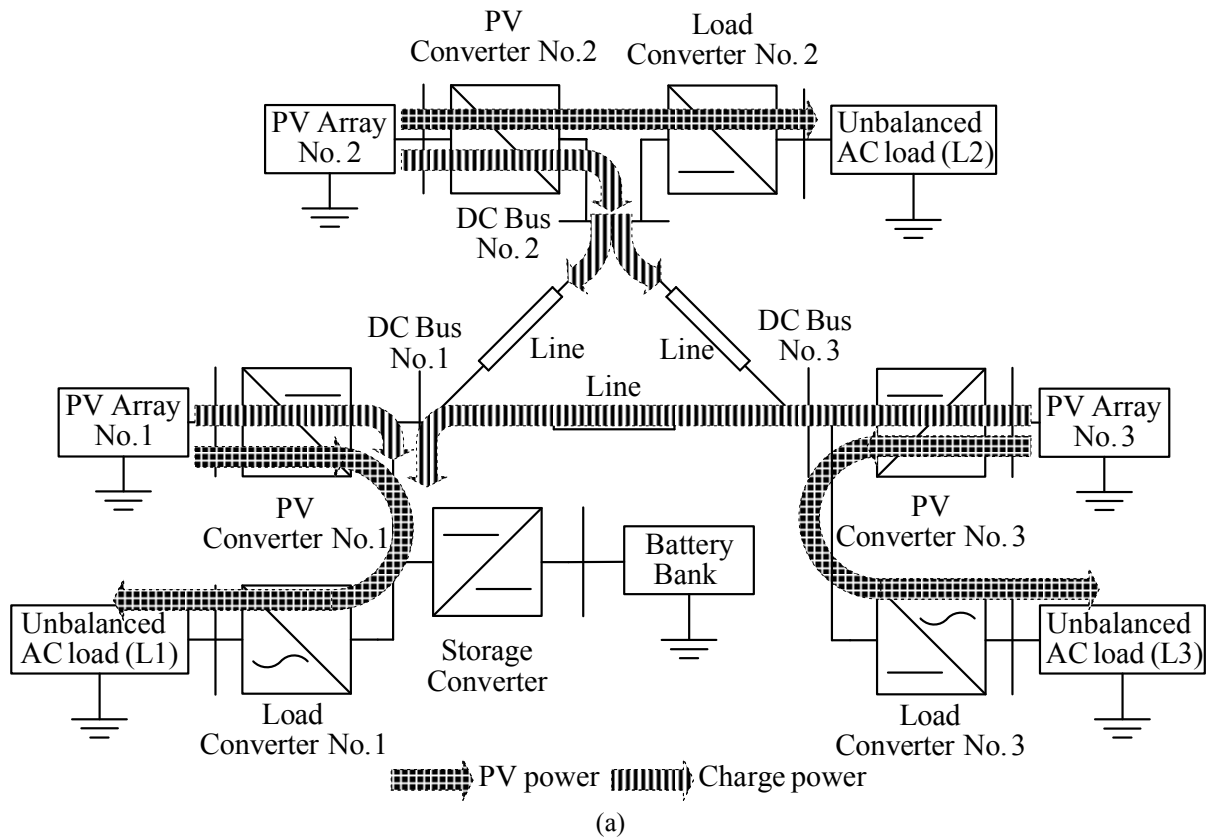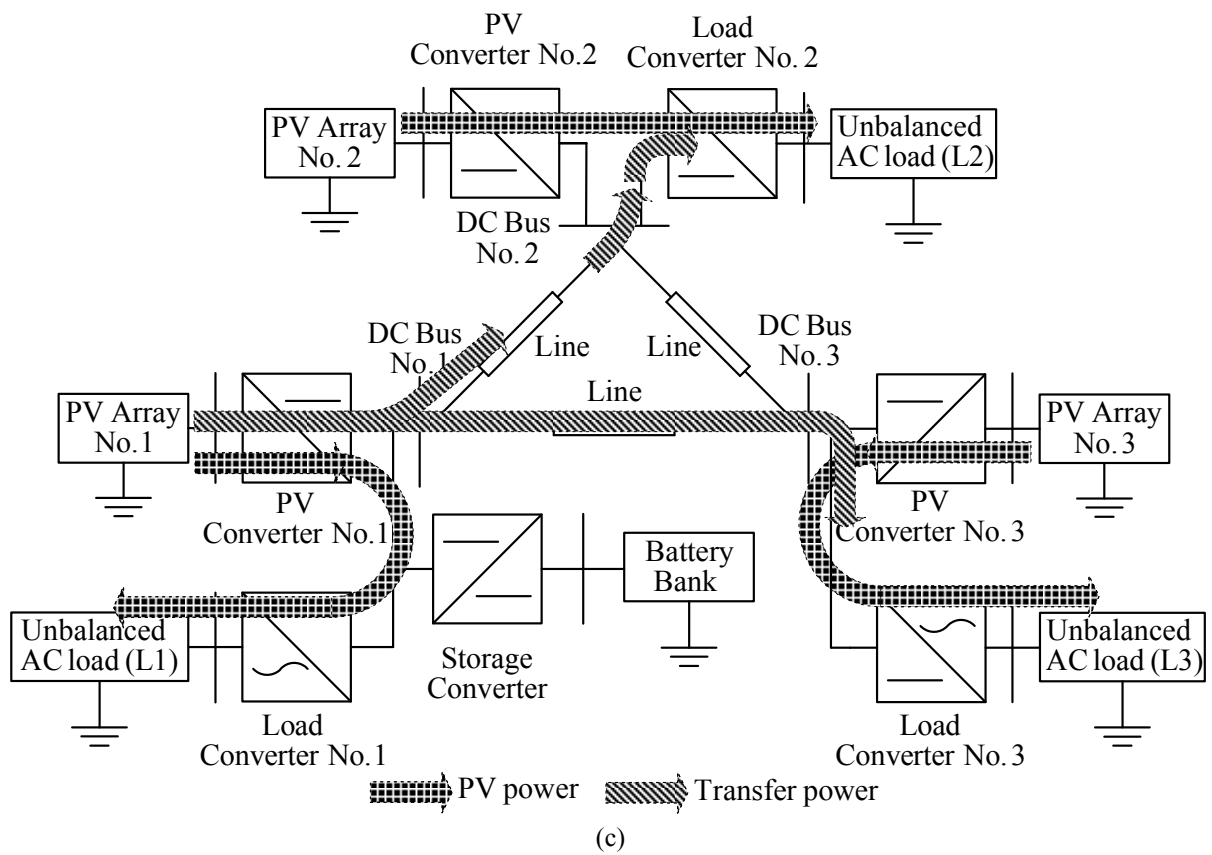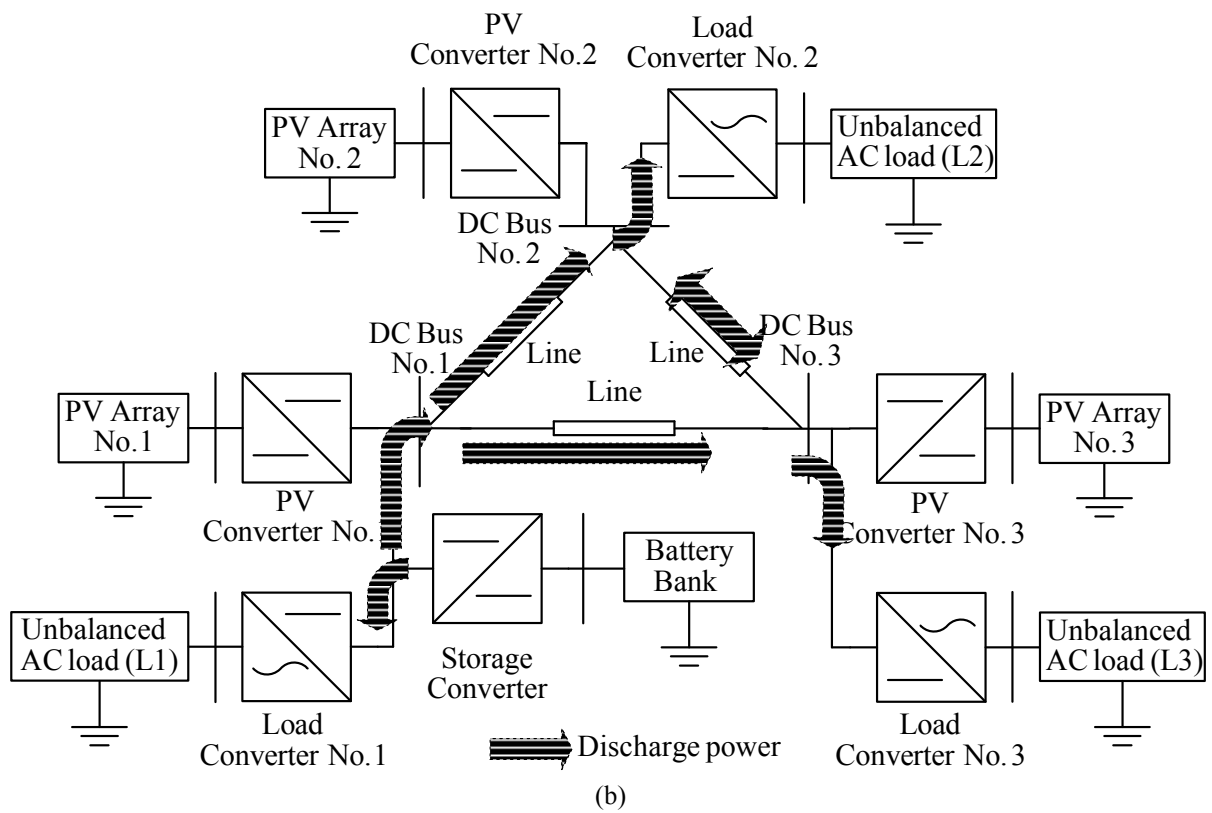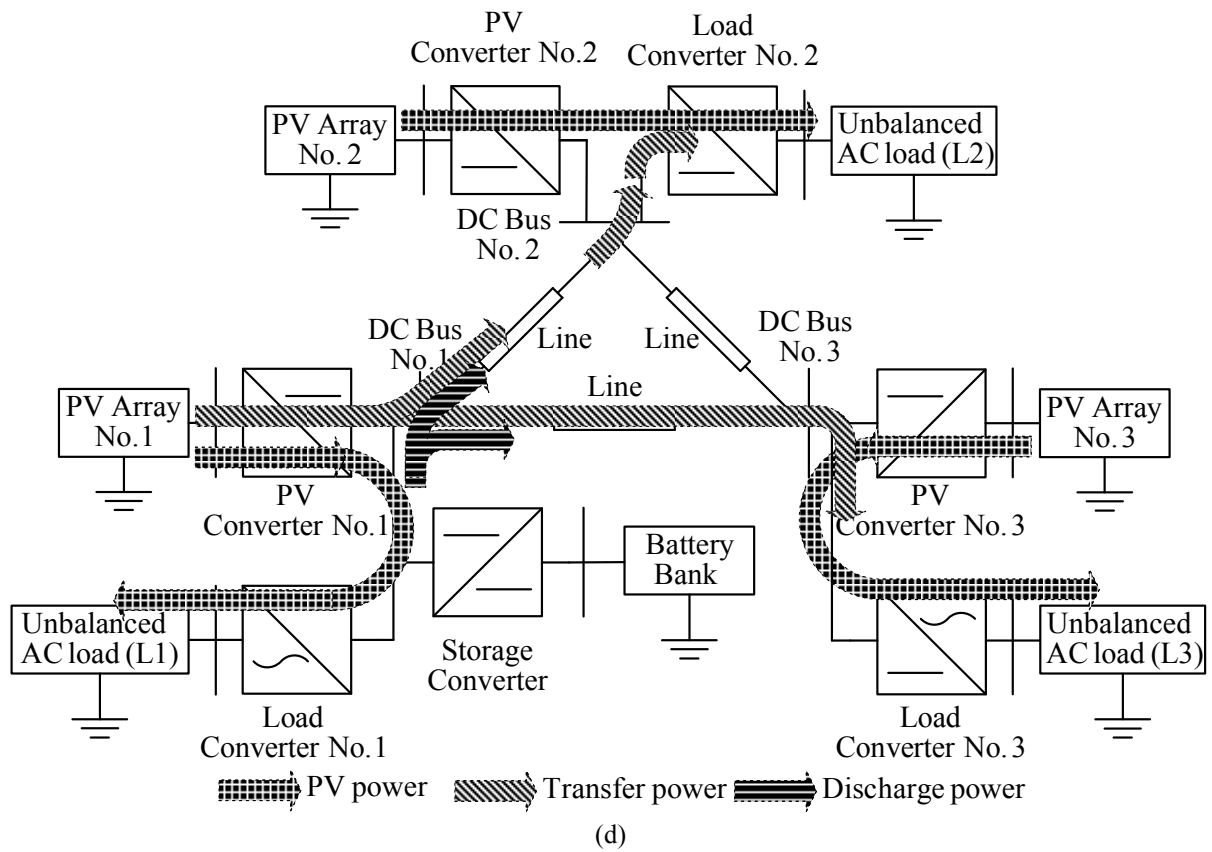
Fig. 2 (a) Daytime mode. (b) Nighttime mode. (c) Daytime excess power transfer mode without discharging battery. (d) Daytime power transfers mode with discharging battery.
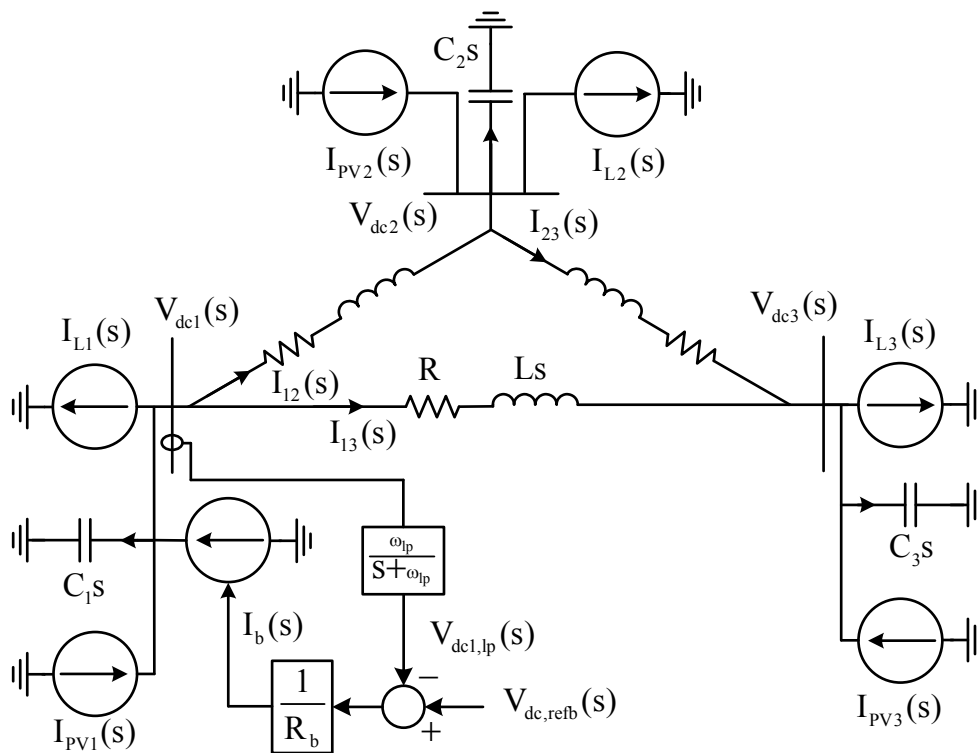
Fig. 3 DC side dynamic model.

Considering equations (1), (2), (3) and (4), the measured DC bus voltages (V_{dc1}, V_{dc2} and V_{dc3}), the reference voltage in DC bus (V_{dcrefb}), output current of the load converters (I_{L1}, I_{L2} and I_{L3}) and output current of the PV converters (I_{PV1}, I_{PV2} and I_{PV3}) can be presented in one block diagram as shown in Fig. 4. This figure shows the main structure of the DC voltage droop controller for the storage converter. Also Fig. 4 shows the dynamic properties of the sample proposed DC network. This model is simulated and used for validation of the detailed modeling of the proposed DC distribution network.

The above mentioned equations for the can be written steady state condition as follows:

$$I_b = \frac{V_{dc,refb} - V_{dc1}}{R_b} \tag{5}$$

$$I_b + I_{PV1} - I_{L1} = \frac{V_{dc1} - V_{dc2}}{R} + \frac{V_{dc1} - V_{dc3}}{R} \tag{6}$$

$$I_{PV2} - I_{L2} = \frac{V_{dc2} - V_{dc1}}{R} + \frac{V_{dc2} - V_{dc3}}{R} \tag{7}$$

$$I_{PV3} - I_{L3} = \frac{V_{dc3} - V_{dc1}}{R} + \frac{V_{dc3} - V_{dc2}}{R} \tag{8}$$

Also, we have:

$$I_b = \sum_{i=1}^{3} I_{Li} - \sum_{i=1}^{3} I_{PVi} \tag{9}$$

Considering equation (9), it is clear that each load demand matches the size of its own PV arrays. The power losses in the proposed system have been reduced and improved utilization. For P_b, we obtain:

$$P_b = V_{dc1} I_b = \frac{V_{dc1}(V_{dc,refb} - V_{dc1})}{R_b} \tag{10}$$

P_b is output DC power of the storage converter. The voltage droop, δ, can be defined as follows:

$$\delta = \frac{V_{dc,refb} - V_{dc1}}{V_{dc,refb}} \tag{11}$$

The equation (10) can be rewritten in the following form:

$$P_b = \frac{\delta(1-\delta)V_{dc,refb}^2}{R_b} \tag{12}$$

At rated power conditions, equation (12) can be rewritten as follows:

$$P_{b,rated} = \frac{\delta_n(1-\delta_n)V_{dc,refb}^2}{R_b} \tag{13}$$

$$R_b = \frac{\delta_n(1-\delta_n)V_{dc,refb}^2}{P_{b,rated}} \tag{14}$$

Figure 5 shows the steady state droop characteristic of storage converter. The output current of this converter can be controlled by the slope of the voltage droop characteristic [7-8]. The basis of voltage and power flow control is that a battery with a DC/DC converter can maintain a stable voltage. This DC/DC converter is bi-directional, and the controlled parameter is the voltage on the network side of the converter. However, DC bus voltage is kept within two threshold V_{refbc} and V_{refbd}. Moreover, If the DC bus voltage exceeds the threshold V_{refpv}, the power produced by PV units is cancelled out.

4 Control Strategies of Converters

In the proposed system, the DC bus voltage regulation made by the storage converter. However it is necessary that the storage converter have been exchange power with the DC network and battery bank as a function of the requested load and the power produced by the PV arrays. In this paper, novel control strategies for each converter have been presented. These strategies are mainly based on the control of the DC bus voltage within acceptable limit. Instead, the PV converters are current-controlled as a function of the generated power of the respective devices. Also, the load converters are voltage-controlled as a function of the absorbed power of the AC loads.

4.1 Circuit Configuration and Control Scheme of Energy Storage Units

The equivalent circuit of the storage converter is shown in Fig. 6. This converter is represented with ideal current source i_{fb}^{ref}. The converter manages the amount of active power exchanged between the DC bus and battery bank. The storage system unit is composed by secondary battery bank. E_{bat} and R_{bat} are the thevenin resistance and voltage of the battery storage bank. As it can be seen in Fig. 6, the input signals of storage converter controller are the battery bank output voltage v_b, output current i_b, the output current for this converter i_{fb}, DC bus voltage v_{dc} and reference DC voltage $V_{dc,refb}$. The circuit configuration and control scheme for storage converter has been depicted in Fig. 7. The storage converter is bidirectional DC/DC converter. This converter has Insulated Gate Bipolar Transistor (IGBT) switches and has been controlled by Pulse-Width Modulation (PWM) voltage controller. The

main part of this scheme is DC voltage regulator based droop controller. It is obvious that the DC voltage error can be fed to the droop controller whose droop is K_b, in order to obtain the injected current (i.e., i_b) to the DC bus. The multiplication of v_{dc} and i_b determines the injected power to the DC bus of storage converter (i.e., p_b). For the DC voltage regulator shown in Fig. 7, we have:

$$i_b = K_b(V_{dc,refb} - v_{dc,lp}) \tag{15}$$

$$p_b = v_{dc}i_b \tag{16}$$

Using equations (15) and (16), we obtain:

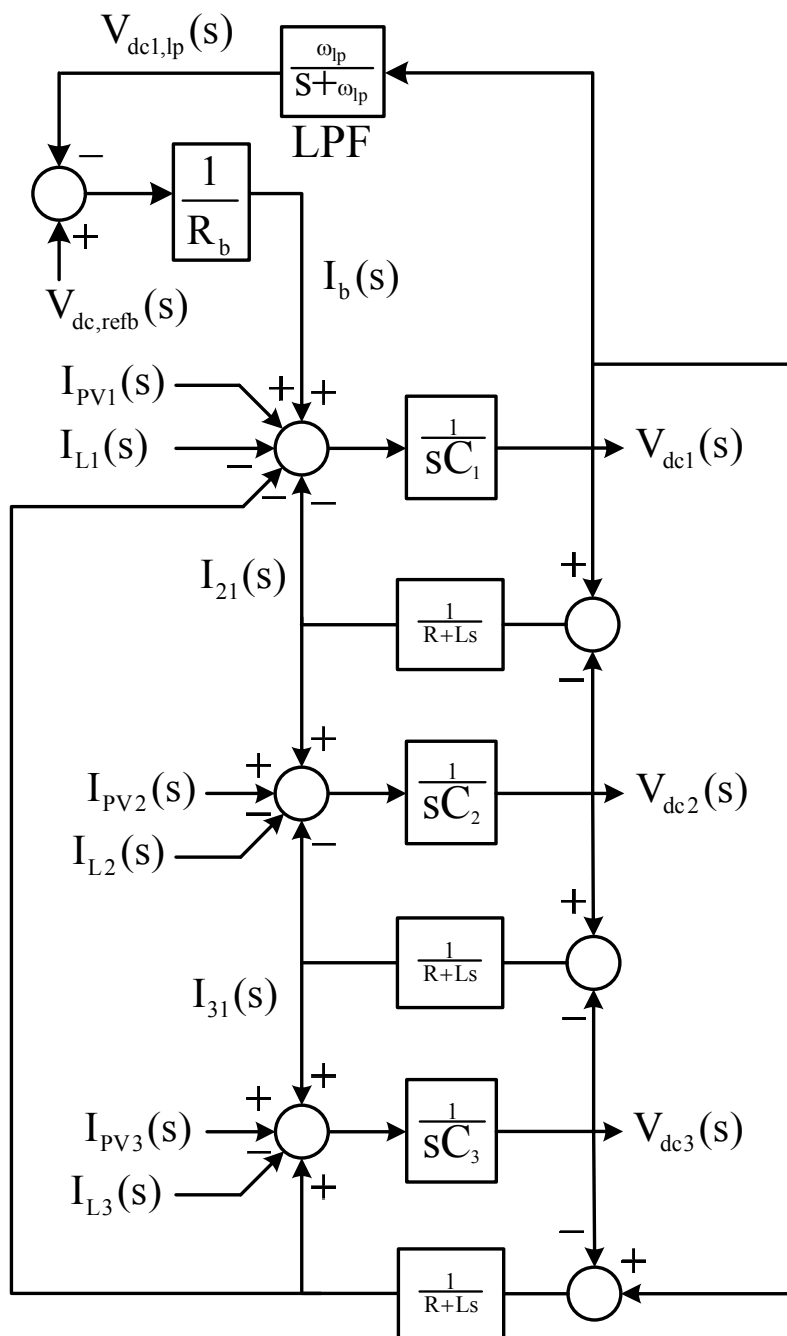$$p_b = K_b v_{dc}(V_{dc,refb} - v_{dc,lp}) \tag{17}$$

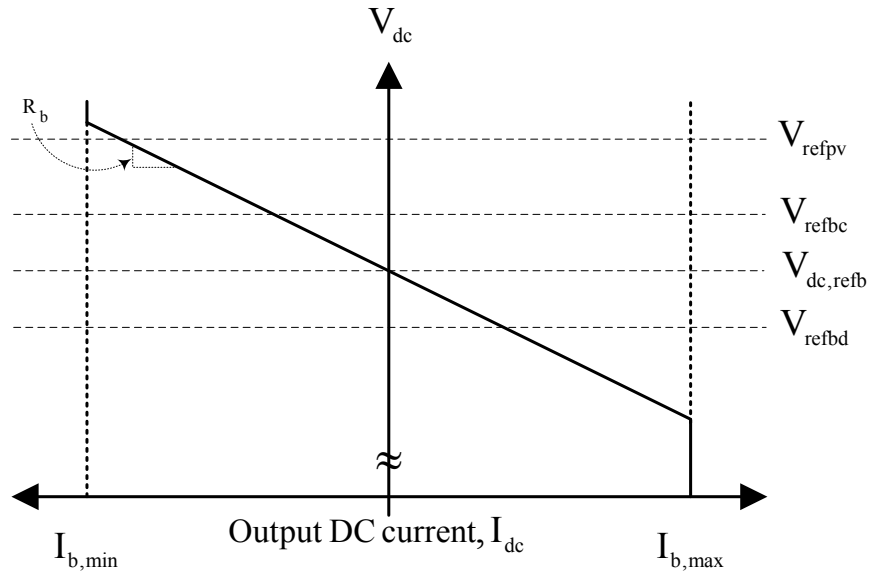Fig. 4 Structure of the DC bus voltages droop controller.

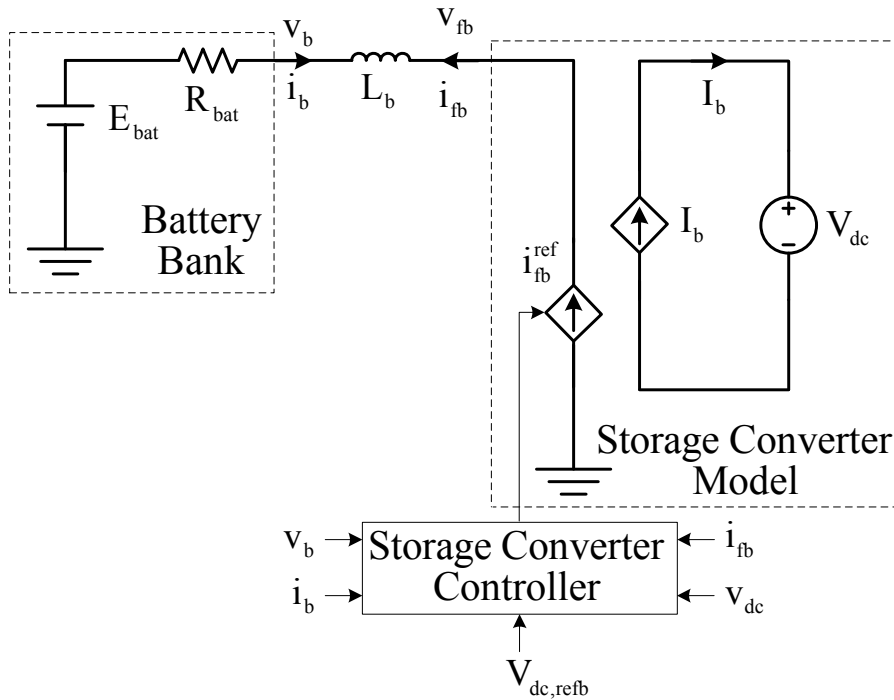**Fig. 5** Droop characteristics of storage converter.

Fig. 6 Equivalent circuit of the storage converter.

The above mentioned equations in steady state condition can be written as follow:

$$I_b = K_b (V_{dc,refb} - V_{dc}) \qquad (18)$$

$$P_b = I_b V_{dc} \qquad (19)$$

$$P_b = K_b V_{dc} (V_{dc,refb} - V_{dc}) \qquad (20)$$

Considering the equations (10) and (20), the steady state droop is:

$$R_b = \frac{1}{K_b} \qquad (21)$$

K_b is designed based on power rating of battery bank for supplying the load demand in nighttime mode operation.

The start-up of the charging and discharging stages is determined by the control loop of the DC bus voltage. If the DC bus voltage remains between references, V_{refbc} and V_{refbd}, the signal p_b is zero, and the storage converter does not exchange power with the DC bus. Also the power required from the loads is entirely supplied by PV arrays. If the voltage exceeds the higher reference V_{refbc}, the signal p_b is negative and the power produced by the PV arrays is used to recharge the storage system. If it is below the lower reference V_{refbd}, the signal p_b is positive and the power stored in battery bank is used to discharge the storage system. However, in the battery energy storage unit, the DC voltage regulator (shown in Fig. 7) makes the power (p_b). The reference current, i_{fb}^{ref}, can be obtained as:

$$i_{fb}^{ref} = -\frac{p_b}{v_b} \qquad (22)$$

where, v_b is battery terminal voltage. This current is limited by upper and lower limits ($I_{b,max}$ and $I_{b,min}$) for the management of the maximum and minimum energy storage in battery bank, and that determines the state of charging or discharging under different operating conditions. In Fig. 7, the reference current, i_{fb}^{ref} and measured filter current, i_{fb}, are fed to the PWM current control box which determines the switching pattern of bidirectional storage converter.
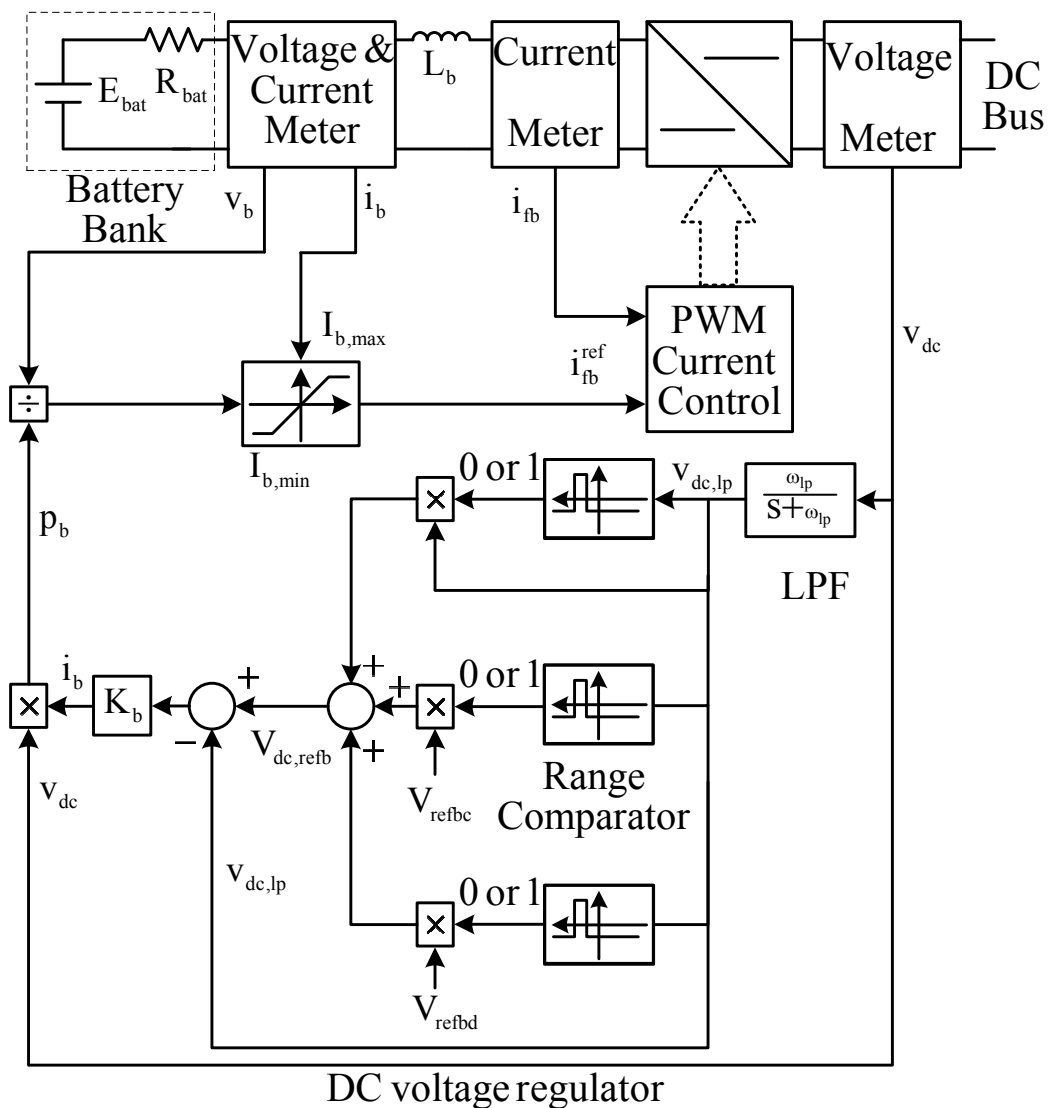

Fig. 7 The circuit configuration and control scheme for storage converter.

4.2 Circuit Configuration and Control Scheme of PV System

Several PV modules are connected in a series and parallel in an array to obtain a suitable power rating. Also the PV cells are connected in a series and parallel in a module. The most commonly used model for a PV cell is the DC current source (I_L) with a diode connected in parallel shown in Fig. 8 [9]-[10]. The DC source current is dependents on ambient temperature (T_a) and solar irradiation (G_a). Resistance R_s represents the losses in the circuit. In this paper, PV dynamic model, reported in [11], is used to model the PV arrays. The PV array can be modeled as voltage/current sources with the $V-I$ characteristic dependent on temperature and irradiation. Since a PV array operates at different weather conditions the optimal operating point changes with irradiation and ambient temperature. Therefore optimal operating voltage has to be applied to achieve the maximum power. This can be done by using a maximum power point tracking (MPPT) algorithm [12]-[13]. In this study a suitable voltage-based MPPT controller for optimum operation of PV arrays has been used. A 200-W PV data (SPR-200-BLK) is used to PV array parameters [14].

The equivalent circuit of a PV array and converter is shown in Fig. 9. This converter is represented with a ideal current source, i_{fpv}^{ref}. The converter manages the amount of current injected to the DC network. As it can be seen in Fig. 9, the input signals of PV converter controller are the PV array output voltage, v_{pv}, the output current, i_{pv}, reference active power of PV array $P_{pv,ref}$, DC bus voltage v_{dc}, and reference DC voltage for PV array, V_{refpv}. The PV array is modeled by a voltage source v_{pv}. The source is controlled by the reference active power for PV array $P_{pv,ref}$.

The configuration and control scheme for PV converter has been shown in Fig. 10. In this control scheme, the reference active power, $P_{pv,ref}$ is specified by the related active power management strategy. The reference current, i_{fpv}^{ref}, can be determined as follow:

$$i_{fpv}^{ref} = -\frac{P_{pv,ref}}{v_{pv}} \tag{23}$$

The comparison of the calculated reference current i_{fpv}^{ref}, and the actual current generated by the PV converter i_{fpv} will result in the error signal, which is fed to the PWM current control box which determines the switching pattern of DC/DC converters.
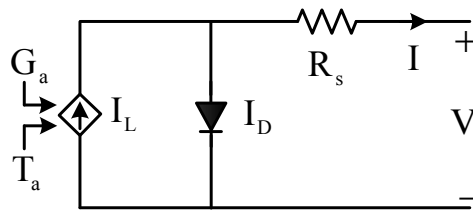

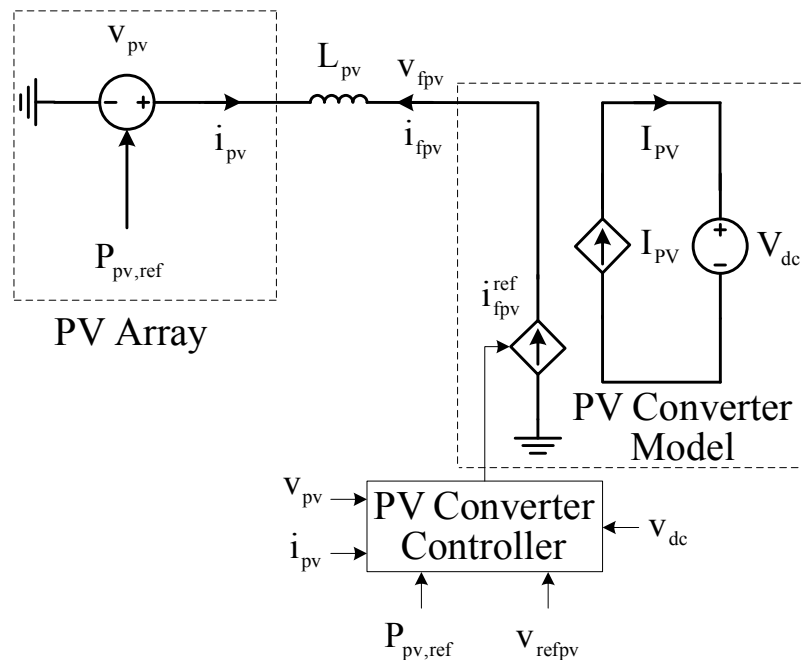**Fig. 8** Model for a single PV cell.

Fig. 9 Equivalent circuit of the PV generation unit.
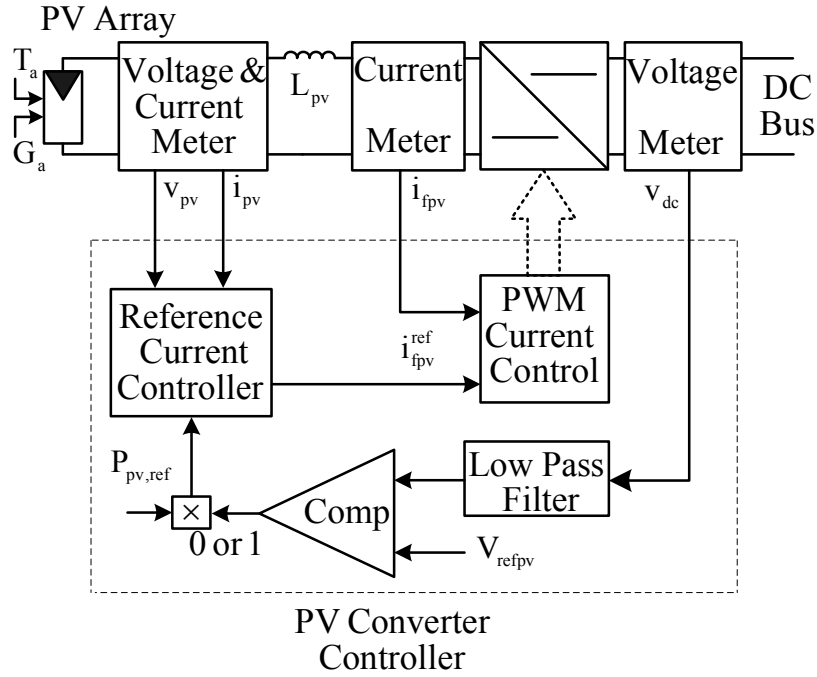
PV Converter
Controller

Fig. 10 Circuit configuration and control scheme for PV converter.

4.3 Circuit Configuration and Control Scheme of AC Loads Connected to the DC Bus

The load converter is voltage source converter (VSC) with neutral clamped DC capacitors. This topology is characterized by the connection of the neutral point of the load to the midpoint of the clamped DC capacitors. The equivalent circuit of the load converter is shown in Fig. 11. This converter is represented with three voltage sources, v_{fa}^{ref}, v_{fb}^{ref} and v_{fc}^{ref}. The equations describing load converter voltages and currents are expressed by the following equation:

$$\begin{bmatrix} v_{fa} \\ v_{fb} \\ v_{fc} \end{bmatrix} = \begin{bmatrix} v_{la} \\ v_{lb} \\ v_{lc} \end{bmatrix} + \begin{bmatrix} L_f & 0 & 0 \\ 0 & L_f & 0 \\ 0 & 0 & L_f \end{bmatrix} \frac{d}{dt} \begin{bmatrix} i_{fa} \\ i_{fb} \\ i_{fc} \end{bmatrix} \quad (24)$$

where, v_{fa}, v_{fb} and v_{fc} are the line to neutral three phase output voltages of the load converter. i_{fa}, i_{fb} and i_{fc} are the three phase output currents. v_{la}, v_{lb} and v_{lc} are the line to neutral three phase voltages of the unbalanced AC loads. The voltage equations in the $d-q-0$ reference frame are as follows [6]:

$$\begin{bmatrix} v_{fd} \\ v_{fq} \\ v_{f0} \end{bmatrix} = \begin{bmatrix} v_{ld} \\ v_{lq} \\ v_{l0} \end{bmatrix} + \begin{bmatrix} L_f & 0 & 0 \\ 0 & L_f & 0 \\ 0 & 0 & L_f \end{bmatrix} \frac{d}{dt} \begin{bmatrix} i_{fd} \\ i_{fq} \\ i_{f0} \end{bmatrix}$$
$$+ \begin{bmatrix} 0 & -\omega L_f & 0 \\ \omega L_f & 0 & 0 \\ 0 & 0 & 0 \end{bmatrix} \begin{bmatrix} i_{fd} \\ i_{fq} \\ i_{f0} \end{bmatrix} \quad (25)$$

The circuit configuration and control scheme for each converter has been depicted in Fig. 12. The DC/AC load

converter between the DC bus and unbalanced AC loads can be controlled by $V-f$ control strategy, which regulates the voltage and the frequency of AC loads. These converters have no loop to regulate the DC bus voltage. In the $V-f$ controller, it is clear that:
a) Frequency (ω) can be obtained by Phase Lock Loop (PLL) using desirable frequency (e.g., 50 Hz).
b) The load phase voltages (v_{la}, v_{lb} and v_{lc}) can be detected and transformed into a $d-q-0$ synchronously rotating reference frame using following equations:

$$\begin{bmatrix} v_{ld} \\ v_{lq} \\ v_{l0} \end{bmatrix} = T_{dq0} \begin{bmatrix} v_{la} \\ v_{lb} \\ v_{lc} \end{bmatrix} \quad (26)$$

$$T_{dq0} = \frac{2}{3} \begin{bmatrix} \cos(\omega t) & \cos(\omega t - 120^\circ) & \cos(\omega t + 120^\circ) \\ -\sin(\omega t) & -\sin(\omega t - 120^\circ) & -\sin(\omega t + 120^\circ) \\ \frac{1}{2} & \frac{1}{2} & \frac{1}{2} \end{bmatrix}$$

The load phase voltage should be kept balanced and sinusoidal with constant amplitude and frequency. Therefore the expected load voltage in the $d-q-0$ reference frame should have only the following value:

$$\begin{bmatrix} v_{ld}^{exp} \\ v_{lq}^{exp} \\ v_{l0}^{exp} \end{bmatrix} = \begin{bmatrix} 0 \\ 0.4\sqrt{\frac{2}{3}} \\ 0 \end{bmatrix} \quad (27)$$
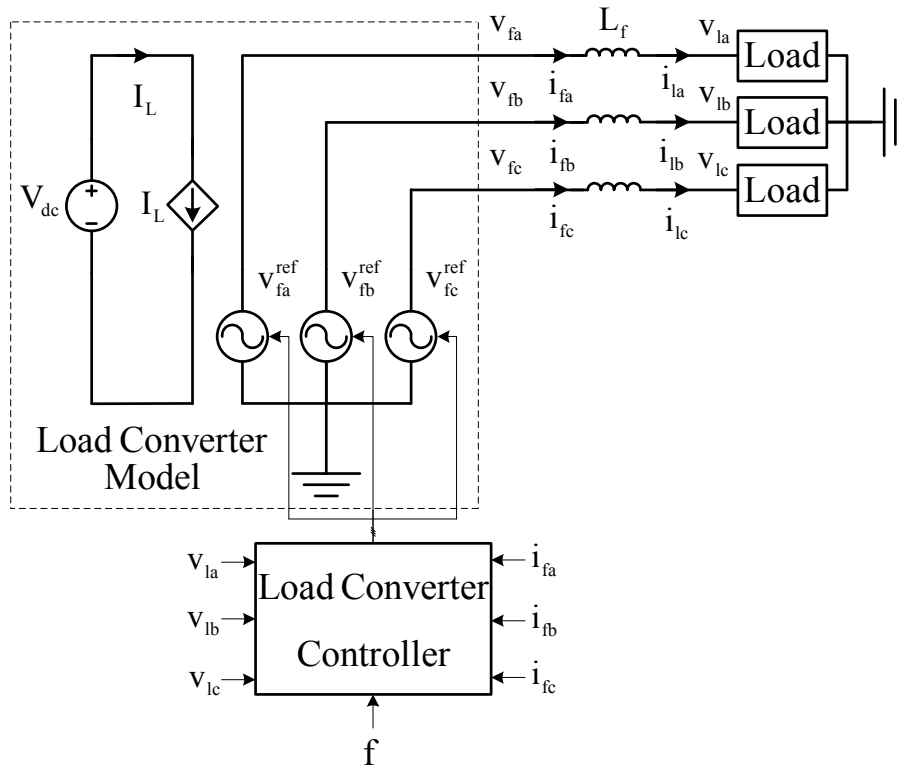
Fig. 11. Equivalent circuit of a load converter.

The load converter controller based on $d-q-0$ rotating reference frame consists of an inner current loop and an outer voltage loop in a three channel arrangement. The current and voltage loops include independent PI controllers for the d, q and 0 channels to eliminate steady state error. The reference load current loops in the $d-q-0$ coordinate are:

$$\begin{bmatrix} i_{ld}^{ref} \\ i_{lq}^{ref} \\ i_{l0}^{ref} \end{bmatrix} = \begin{bmatrix} PI(v_{ld} - v_{ld}^{exp}) \\ PI(v_{lq} - v_{lq}^{exp}) \\ PI(v_{l0} - v_{l0}^{exp}) \end{bmatrix} \qquad (28)$$

The output signals from PI controller can be expressed by the equation (29).

$$\begin{bmatrix} v_{fd}^{ref} \\ v_{fq}^{ref} \\ v_{f0}^{ref} \end{bmatrix} = \begin{bmatrix} v_{ld} \\ v_{lq} \\ v_{l0} \end{bmatrix} + \begin{bmatrix} PI(i_{ld}^{ref} - i_{fd}) \\ PI(i_{lq}^{ref} - i_{fq}) \\ PI(i_{l0}^{ref} - i_{f0}) \end{bmatrix} + \begin{bmatrix} -\omega L_f i_{fq} \\ \omega L_f i_{fd} \\ 0 \end{bmatrix} \qquad (29)$$

The reference output voltages for the load converter are transformed to the $a-b-c$ by using inverse synchronously rotating and stationary reference frames.

$$\begin{bmatrix} v_{fa}^{ref} \\ v_{fb}^{ref} \\ v_{fc}^{ref} \end{bmatrix} = T_{abc} \begin{bmatrix} v_{fd}^{ref} \\ v_{fq}^{ref} \\ v_{f0}^{ref} \end{bmatrix} \qquad (30)$$

$$T_{abc} = \begin{bmatrix} \cos(\omega t) & \sin(\omega t) & 1 \\ \cos(\omega t - 120^\circ) & \sin(\omega t - 120^\circ) & 1 \\ \cos(\omega t + 120^\circ) & \sin(\omega t + 120^\circ) & 1 \end{bmatrix}$$

Then the available voltages in the $a-b-c$ coordinate are compared with the triangular wave provided by PWM voltage control box. Therefore the output provides suitable switching pattern of each load converter.

5 Simulation Results

The system shown in Fig. 1 has been modeled and simulated by PSCAD/EMTDC software in order to study the response of the isolated DC network (associated with PV arrays) to power quality problems. The proposed control methods for power electronic interfaces have been modeled using the same software. The simulation results show that the proposed system is able to supply high quality AC and DC voltages to all loads supplied by the DC network.

In the simulation studies it is assumed that 100 kW storage converter is in service. It is also assumed that the reference DC voltage is 750 V and the nominal

droop is 5 percent. The rated power for each PV array is assumed to be 50 kW. The rated power for each unbalanced AC load is assumed to be 25 kW.

The ambient temperature (T_a) is assumed to 20 °C. For the purpose of simulation, the solar irradiance, G_a has been shown in Fig. 13.

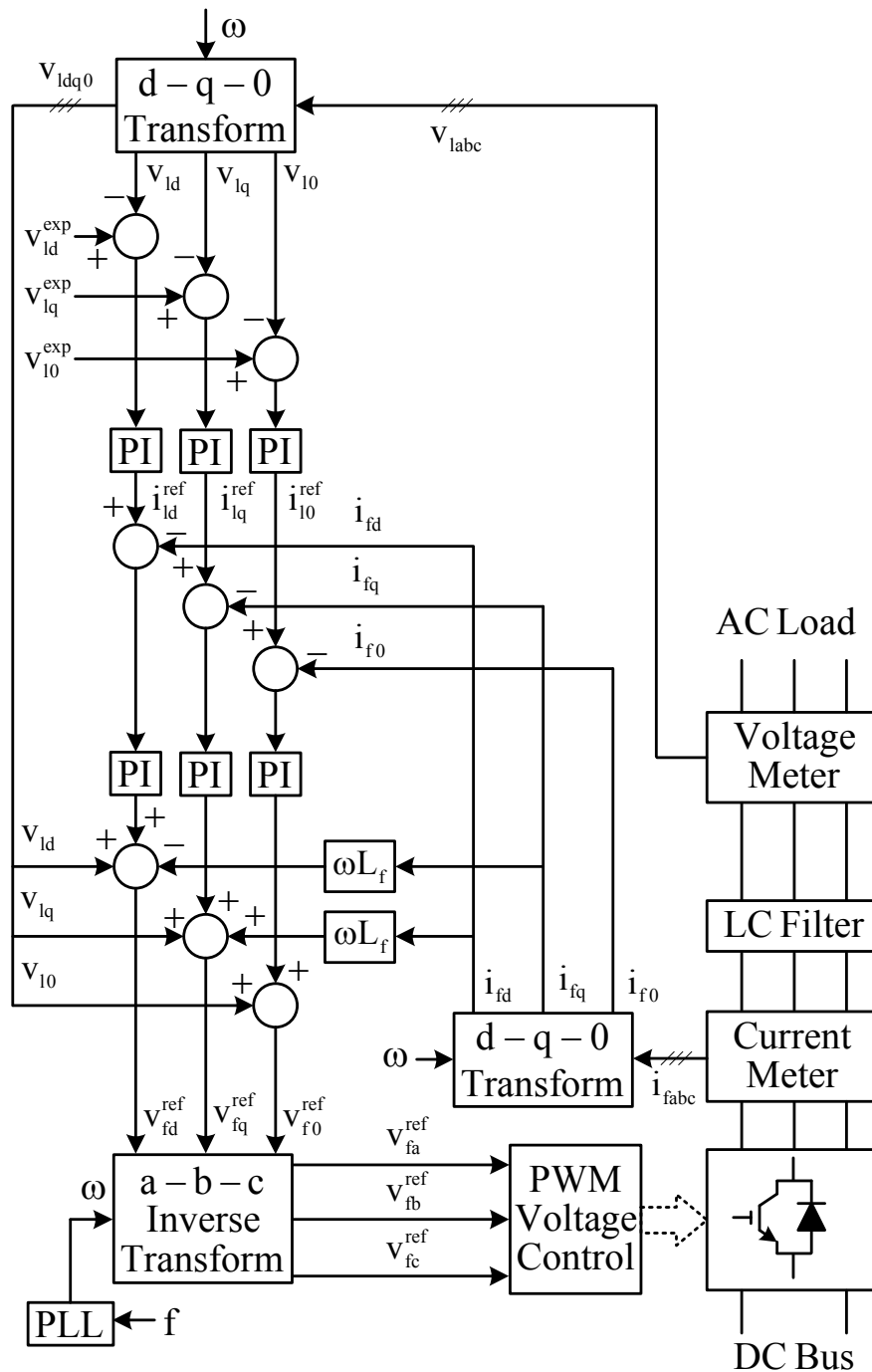**Fig. 12** Circuit configuration and control scheme for load converter.

As shown in Fig. 13, the irradiance has been changed from $1.5\cos(2\pi t)\,kW/m^2$ to zero at $t = 1.25s$ and then from zero to $1.5\cos(2\pi t)\,kW/m^2$ at $t = 1.75s$. When $0.75 < t < 1.25s$ and $1.75 < t < 2.25s$, the all PV arrays are operated in daytime mode. When $0.5 < t < 0.75s$,

$1.25 < t < 1.75s$ and $2.25 < t < 2.5s$, all PV arrays are operated in nighttime mode. Simulation results show the transfer power with charging and discharging the battery bank in DC network.

Fig. 14 shows the instantaneous active power of the energy storage unit (P_b), all PV arrays ($P_{PVs} = P_{PV1} + P_{PV2} + P_{PV3}$) and all unbalanced AC loads ($P_{Ls} = P_{L1} + P_{L2} + P_{L3}$). It can be said that the suggested control strategy for PV converters provides reasonable response. In the daytime charging mode, the PV power is larger than the load demand. However the excess power charges the battery bank as shown in Fig. 14. Nighttime discharging mode, The PV power is absent and only the battery bank supplies the loads as shown in Fig. 14. Also the instantaneous active power of storage converter (P_b) has been varied corresponding to the DC reference voltage and equivalent resistance of the storage converter. Fig. 14 also shows that the consumed power by unbalanced AC loads is constant.

Fig. 15 shows the power transfer in cable connected among each PV arrays with charging and discharging the battery bank. It is observed that the powers P_{12} and P_{13} have been exchanged between battery bank and PV units No. 2 and No. 3 in the nighttime and daytime operating conditions, respectively. The power P_{23} has been exchanged between bus No. 2 and No. 3. As shown in Fig. 13, the power transfer P_{23} is zero.

Figure16 depict the voltage of DC bus No. 1, No. 2 and No. 3, which experiences a swell while the PV power

generated has been increased and returns to the nominal DC voltage. It is also clear that when the PV power generated has been decreased, the DC network voltage experiences sag phenomena. As it can be seen the DC bus voltages (V_{dc1} , V_{dc2} and V_{dc3}) follows the DC voltage ($V_{dc1,dy}$, $V_{dc2,dy}$ and $V_{dc3,dy}$) calculated dynamic properties in Fig. 4, which matches together. The other simulation results which are not presented in this paper can be verified by equations (10) and (20). Fig. 17 shows the phase currents of unbalanced AC load (L1). It was found that the load phase currents are not sinusoidal. Figures 18, 19 and 20 illustrate the phase voltages at the terminal of the unbalanced AC loads (V_{aL1} , V_{bL1} and V_{cL1}), (V_{aL2} , V_{bL2} and V_{cL2}), and (V_{aL3} , V_{bL3} and V_{cL3}), respectively. It is obvious that the balanced voltages are provided for the unbalanced AC load while the load phase currents are not sinusoidal. To quantify the level of the voltage unbalance, the percentage of unbalance is expressed in accordance with the definition of the "degree of unbalance in three phase system" [15]. In this case, the negative sequence unbalance is lower then 1% which is acceptable. It must be noticed that international standards admit unbalances lower than 2% [15].
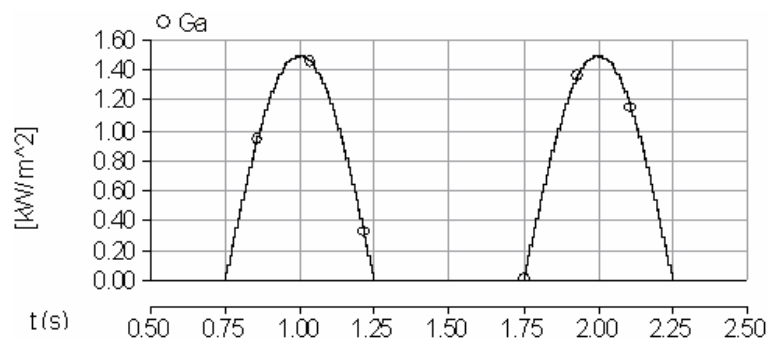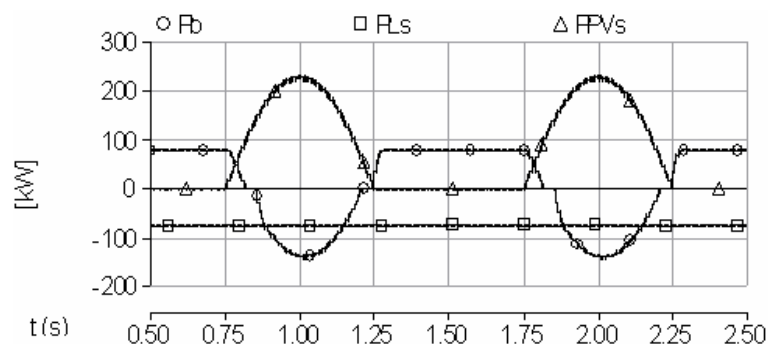

Fig. 13 solar irradiance.
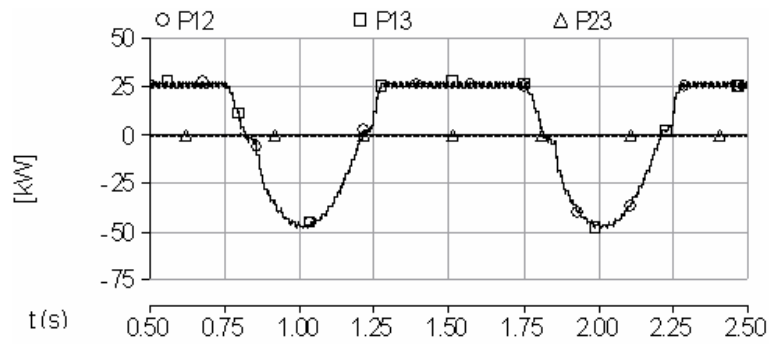

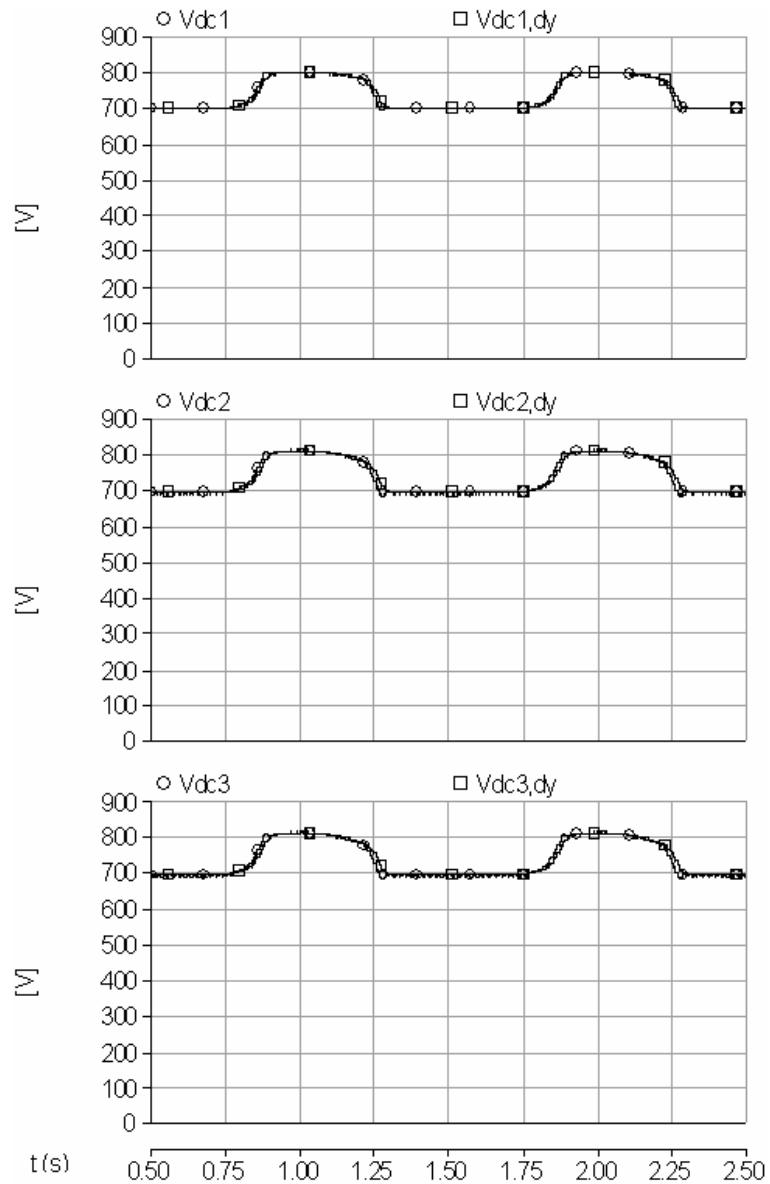**Fig. 14** Active power variations.

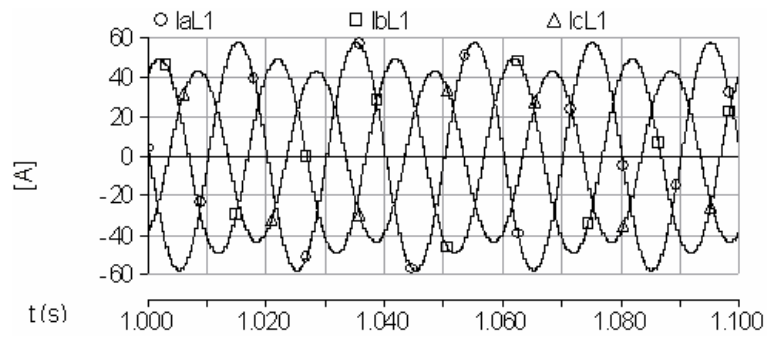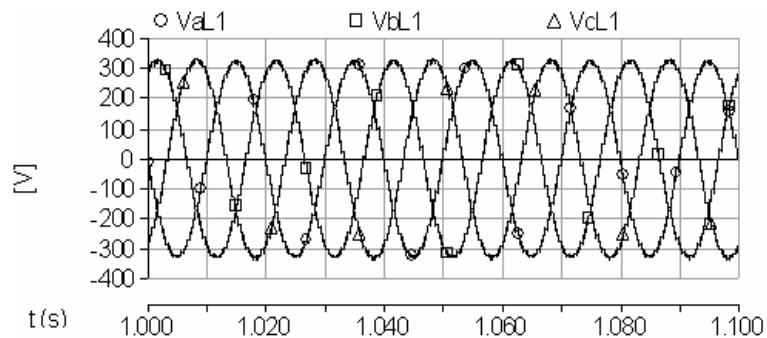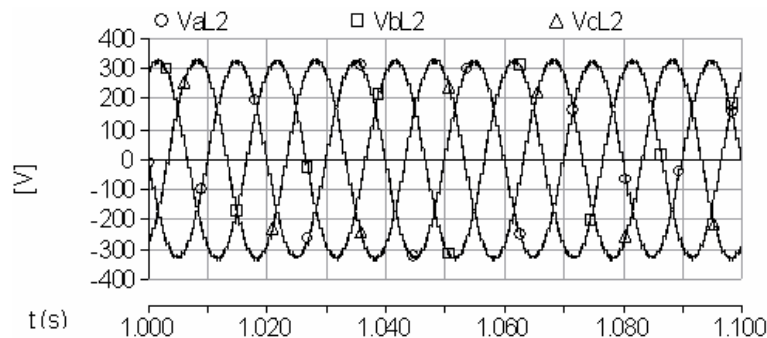**Fig. 15** Power transfer in cable connected among each PV units.
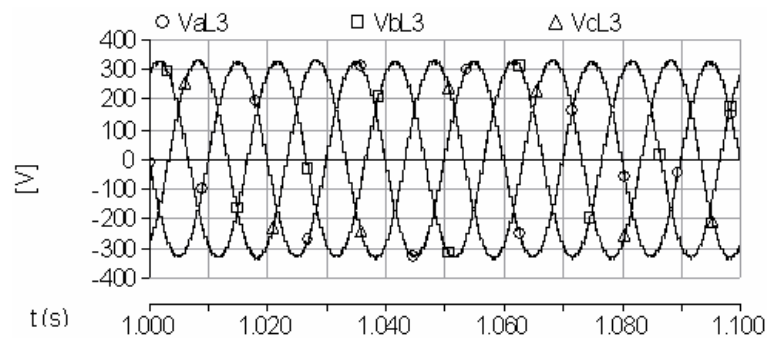

Fig. 16 DC network voltages.

Fig. 17 Unbalanced AC load phase currents.

Fig.18 Phase voltages in AC side of load converter No. 1 (L1).

Fig.19 Phase voltages in AC side of load converter No. 2 (L2).

Fig. 20 Phase voltages in AC side of load converter No. 3 (L3).

6 Conclusion

This paper demonstrates the DC isolated loop network which is fed by PV systems for supplying unbalanced AC loads. We made the main concept of the power management strategy, and then, on the power flow and voltage control. In this paper PSCAD/EMTDC software has been used for the modeling and the simulation of the system component and proposed control strategies for power electronic interfaces, in order to investigate the DC network voltage behaviors, power quality problems and high reliability. The results show that the proposed strategies provide the suitable load sharing between DC/DC converters in order to achieve optimized plant management, while the DC network voltage remains with acceptable level. The paper shows that a DC network with PV system is very realistic and more reliable. The results also show that the proposed system can supply the unbalanced AC load with balanced voltages. It is shown that the unbalancing would not be occurred in the DC network by the unbalanced AC load. Finally, we believe that isolated DC network with distributed generation from renewable sources could be one of the most promising alternatives for the supplying the stand alone loads, where villages are often far away from the utility grid.

7 List of Abbreviations and symbols

7.1 Abbreviations

DG	distributed generations
PV	photovoltaic
VSC	voltage source converters
IGBT	insulated gate bipolar transistor
PWM	pulse-width modulation
MPPT	maximum power point tracking
PLL	phase lock loop

7.2 Symbols

a, b, c	phase order in a-b-c coordinate
d, q, 0	phase order in d-q-0 coordinate
$V_{dc,refb}$	DC reference voltage of the storage converter
I_b	output current of the storage converter
P_b	output DC power of the storage converter
R_b	equivalent resistance of the storage converter
K_b	controller gain for storage converter
P_{PVn}	output power of n-th PV units
P_{pvs}	output power of the all PV arrays
P_{Ln}	power consumed n-th AC loads
P_{Ls}	power consumed of the all loads
$P_{pv,ref}$	reference active power for each PV unit
i_{fpv}^{ref}	reference current for each PV unit
v_{fi}^{ref}	reference current for each load converter for phase i
f	frequency in general
v_i	instantaneous line/neutral voltage for phase i
i_i	instantaneous phase current for phase i

References

[1] Azbe V. and Mihalic R., "Distributed generation from renewable sources in an isolated DC network," *Renewable Energy*, Vol. 31, No. 14, pp. 2370-2384, 2006.

[2] Agustoni A., Brenna M. and Tironi E., "Proposal for a High Quality DC Network with Distributed Generation," *in Proc. of 17-th International Conference on Electricity Distribution CIRED*, Barcelona, May 2003.

[3] Dakkak M., Hatori K., and Ise T., "The concept of distribution flexible network PV system," *Renewable Energy*, Vol. 31, pp. 1916–1933, 2006.

[4] Lin B. R. and Lee Y. C., "Three-phase power quality compensator under the unbalanced sources and nonlinear loads," *IEEE Trans. Power Electronics,* Vol. 51, No. 5, pp. 1009–1017, October 2004.

[5] Blazic B. and Papic I., "A new mathematical model and control of D-StatCom for operation under unbalanced conditions," *Electric Power System Research*, Vol. 72, No. 3, pp. 279-287, Dec. 2004.

[6] Vechiu I., Camblong H., Tapia G., Dakyo B. and Curea O., "Control of four leg inverter for hybrid power system applications with unbalanced load," *Energy Conversion and Management*, Vol. 48, pp. 2119–2128, 2007.

[7] Mahmoodi M., Gharehpetian G. B., Abedi M., Noroozian R., "A Suitable Control Strategy for Source Converters and a Novel Load Generation Voltage Control Scheme for DC Voltage Determination in DC Distribution Systems," *in Proc. of First International Power and Energy Conference, PECon 2006*, pp. 363-367, Nov. 2006, Putrajaya, Malaysia.

[8] Karlsson P., Svensson J. "DC network Voltage Control for a Distributed Power System," *IEEE Trans. Power Electronics*, Vol. 18, No. 6, pp. 1405-1412, Nov. 2003.

[9] Patel M. R., *Wind and Solar Power Systems*, CRC Press, 1999.

[10] Gow J. A. and Manning C. D., "Development of a photovoltaic array model for use in power electronic simulation studies," *IEE Proceedings*

on Electric Power Applications, Vol. 146, No. 2, pp. 193-200, 1999.

[11] Hansen A. D. and Sorensen P., "Models for a Stand-Alone PV system," *Riso National Laboratory*, Roskilde, Denmark, Dec 2000.

[12] Koutroulis E., Kalaitzakis K., and Voulgaris N. C., "Development of a microcontroller-based, photovoltaic maximum power point tracking control system," *IEEE Tran. Power Electronics*, Vo. 16, No. 1, pp. 46-54, 2001.

[13] Hua C. and Shen C., "Study of maximum power tracking techniques and control of DC/DC converters for photovoltaic power system," *Proceedings of the 29th Annual IEEE Power Electronics Specialists Conference*, Vol. 1, pp. 86-93, 1998.

[14] Sun Power Corporation, www.sunpowercorp.com, "Residential PV nodule SPR-200-BLKdatasheet," Dec. 2004.

[15] T. Short, *Electric Power Distribution Handbook*, CRC Press, 2004.

R. Noroozian was born in Bonab, Iran in 1975. He received his BS and MS from Tabriz University, Tabriz, Iran and Amirkabir University of Technology (AUT), Tehran, Iran, in 2000 and 2003, respectively. Currently he is a PhD student at Amirkabir University of Technology (AUT), Tehran, Iran. His research interests include distributed generation, distribution power system and power quality.
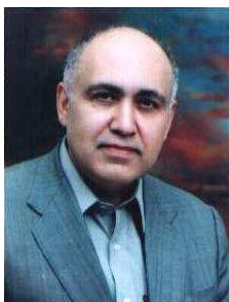
M. Abedi received his B.Sc., M. Sc. and Ph.D. from Tehran University, London University and Newcastle University in 1970, 1973, and 1977, respectively. He worked for G.E.C. (U.K) till 1978. Since then he joined EE Dept of Amirkabir University (Tehran, Iran) where he is now the professor and member of Center of Excellency on Power System. Prof. Abedi has published more than 25 books and 160 papers in journals and conferences. He is distinguished professor in Iran and is prize winner for two outstanding books. He is also member of Iranian Academy of Science and member of CIGRE. His main interest is electrical machines and power systems modeling, operation and control.

G. B. Gharehpetian was born in Tehran, in 1962. He received his BS and MS degrees in electrical engineering in 1987 and 1989 from Tabriz University, Tabriz, Iran and Amirkabir University of Technology (AUT), Tehran, Iran, respectively, graduating with First Class Honors. In 1989 he joined the Electrical Engineering Department of AUT as a lecturer. He received the Ph.D. degree in electrical engineering from Tehran University, Tehran, Iran, in 1996. As a Ph.D. student he has received scholarship from DAAD (German Academic Exchange Service) from 1993 to 1996 and he was with High Voltage Institute of RWTH Aachen, Aachen, Germany. He held the position of Assistant Professor in AUT from 1997 to 2003, and has been Associate Professor since 2004. Dr. Gharehpetian is a Senior Member of Iranian Association of Electrical and Electronics Engineers (IAEEE), member of IEEE and member of central board of IAEEE. Since 2004 he is the Editor-in-Chief of the Journal of IAEEE. The power engineering group of AUT has been selected as a Center of Excellency on Power Systems in Iran since 2001. He is a member of this center and since 2004 the Research Deputy of this center. Since November 2005 he is the director of the industrial relation office of AUT. He is the author of more than 222 journal and conference papers. His teaching and research interest include power system and transformers transients, FACTS devices and HVDC transmission.

S. H. Hosseini was born in Marand, Iran in 1953. He received the M.S. degree from the Faculty of Engineering University of Tabriz, Iran in 1976, the DEA degree from INPL, France, in 1978 and Ph.D. degree from INPL, France, in 1981 all in electrical engineering. In 1982 he joined the University of Tabriz, Iran, as an assistant professor in the Dept. of Elec. Eng., from 1990 to 1995 he was associate professor in the University of Tabriz, since 1995 he has been professor in the Dept. of Elec. Eng. University of Tabriz. From Sept. 1990 to Sept. 1991 he was visiting professor in the University of Queensland, Australia, from Sept. 1996 to Sept. 1997 he was visiting professor in the University of Western Ontario, Canada. His research interests include Power Electronic Converters, Matrix Converters, Active & Hybrid Filters, Application of Power Electronics in Renewable Energy Systems and Electrified Railway Systems, Reactive Power Control, Harmonics and Power Quality Compensation Systems such as SVC, UPQC, FACTS devices.